

Opinion

# Osseoconductive and Corrosion-Inhibiting Plasma-Sprayed Calcium Phosphate Coatings for Metallic Medical Implants

Robert B. Heimann 

Am Stadtpark 2A, D-02826 Görlitz, Germany; robert.heimann@ocean-gate.de; Tel.: +49-(0)-3581-667851

Received: 25 August 2017; Accepted: 22 October 2017; Published: 1 November 2017

**Abstract:** During the last several decades, research into bioceramic coatings for medical implants has emerged as a hot topic among materials scientists and clinical practitioners alike. In particular, today, calcium phosphate-based bioceramic materials are ubiquitously used in clinical applications to coat the stems of metallic endoprosthetic hips as well as the surfaces of dental root implants. Such implants frequently consist of titanium alloys, CoCrMo alloy, or austenitic surgical stainless steels, and aim at replacing lost body parts or restoring functions to diseased or damaged tissues of the human body. In addition, besides such inherently corrosion-resistant metals, increasingly, biodegradable metals such as magnesium alloys are being researched for osseosynthetic devices and coronary stents both of which are intended to remain in the human body for only a short time. Biocompatible coatings provide not only vital biological functions by supporting osseoconductivity but may serve also to protect the metallic parts of implants from corrosion in the aggressive metabolic environment. Moreover, the essential properties of hydroxylapatite-based bioceramic coatings including their *in vitro* alteration in contact with simulated body fluids will be addressed in this current review paper. In addition, a paradigmatic shift is suggested towards the development of transition metal-substituted calcium hexa-orthophosphates with the NaSiCON (Na superionic conductor) structure to be used for implant coatings with superior degradation resistance in the corrosive body environment and with pronounced ionic conductivity that might be utilized in novel devices for electrical bone growth stimulation.

**Keywords:** hydroxylapatite; plasma spraying; bioceramic coating; phase composition; Ti6Al4V; Mg alloys; osseoconductivity; adhesion strength; residual stress; corrosion resistance; NaSiCON

## 1. Introduction

Owing to structure and composition close to those of biological bone-forming apatite, synthetic hydroxylapatite ( $\text{Ca}_{10}(\text{PO}_4)_6(\text{OH})_2$ ; HAp) is widely being used as biomedical coating for implants, most frequently to coat the stems of hip endoprostheses and parts of dental root implants. During the past decades, many attempts have been made to optimize essential properties of osseoconductive HAp coatings. Osseoconductivity is defined as the ability of a biomaterial to foster the ingrowth of bone cells, blood capillaries, and perivascular tissue into the gap between implant and existing (cortical) bone.

Consequently, there was (and is) much research aimed at depositing thin HAp layers by a plethora of surface coating techniques. These techniques include low temperature methods such as biomimetic precipitation from simulated body solutions, wet chemical processing via sol-gel routes, electron and magnetron sputtering, ion beam-assisted deposition (IBAD), electrophoretic deposition (EPD), plasma electrolytic oxidation (PEO), and several other less frequently utilized techniques [1,2]. However, thermal, in particular, plasma spraying is still the method of choice applied by the medical industry to coat the stems of hip endoprostheses [3]. Indeed, such coatings deposited by atmospheric (air)

plasma spraying (APS) of hydroxylapatite powder with particle diameters of tens to hundreds of micrometers is the most popular, and the only Food and Drug Administration (FDA)-approved, method to coat implant surfaces for clinical use. To guarantee optimum performance and sufficient lifetime of implants *in vivo*, plasma-sprayed HAp coatings have to be optimized in terms of adhesion and cohesion strength, phase composition, crystallinity, porosity, surface roughness, residual stress distribution, thickness, and corrosion inhibition capability [4].

## 2. Economic Considerations

Today, development of bioceramic materials is in the vanguard of health-related issues in many countries. Arguably, research into ceramic biomaterials has reached a level of involvement, sophistication, and research investment comparable to electronic ceramics. The reason for this is obvious as worldwide a large proportion of an aging population relies on repair or replacement of body parts or restoration of lost body functions, ranging from implantation of dental roots, to alveolar ridge and iliac crest augmentation, to artificial skin grafts, to hip and knee endoprostheses. As hip and knee arthroplasties using endoprosthetic implants are considered flagships of implantology, the subject of this article will largely revolve around such devices.

At present, in OECD countries such as the United States, Switzerland, and Germany, the utilization rates of hip arthroplasty exceed 200 total hip arthroplasties (THA) per 100,000 population [5,6]. As expected, there is a strong correlation between the gross domestic product (GDP) and health care expenditure per capita with utilization rates [7]. Hence, these rates show much lower values in Spain (102/100,000) and, in particular, Mexico (8/100,000). In Australia, 83 hip arthroplasties per 100,000 population were performed in 2004, substantially increasing to 104 per 100,000 population in 2014 [8]. This high and growing demand is the result of the wear and tear the joints providing the ambulatory kinematics suffer during a human lifetime but is also caused by degenerative diseases such as osteoarthritis, rheumatoid arthritis, and osteoporosis, and damage caused by physical harm from external sources. Not surprisingly, today the worldwide sales of hip and knee orthopaedic surgical joint replacement products are USD 16.7 billion, anticipated to double by 2022 to reach USD 33 billion [9]. This trend is indeed a very strong incentive to embark on research and development aiming at providing novel and improving existing bioceramic osseointegrative coatings for metallic implants.

## 3. Two Types of Metallic Implant

At present, there are two basic types of endoprosthetic devices: commercially available corrosion-resistant implants and experimental implants based on biodegradable Mg and Fe alloys. Sufficiently corrosion-resistant titanium alloys (Ti6Al4V, Ti6Al7Nb, Ti13Nb13Zr and others), CoCrMo alloy, tantalum, and austenitic surgical steels (AISI 136L, AISI 304) are ubiquitously utilized for the shafts of endoprosthetic hip implants, knee implants, dental roots, coronary stents, vascular clips, femoral balls, osteosynthetic plates and bone screws, and several other applications. Besides, medium-entropy magnesium alloys such as AZ31, AZ91, ZK60 or WE43 are currently considered suitable candidate materials for biomedical applications based on their favorable mechanical properties, and their confirmed biocompatibility and osseointegrativity. Hence, such Mg and Fe alloys could potentially be utilized for osteosynthetic musculoskeletal fixating devices [10] that include fracture fixation screws and plate systems for use in extremity locations, interference screws, surgical clips, screws for femoral head fixation, spinal implants and cages, and others. Moreover, substantial research is underway to improve bioresorbable cardiovascular stents based on Mg alloys that are being designed to provide short-term supporting structures for vascular implants to combat coronary heart and peripheral artery diseases [11–13].

Despite successful efforts to improve the *in vivo* performance of osseosynthetic bone fixation devices and cardiovascular stents based on Mg alloys, there is the ultimate challenge for future medical product development: use of Mg alloys for endoprosthetic hip and knee implants. The combination of novel Mg alloys and ever more sophisticated surface modification processes to deposit a corrosion

resistant coating has created the potential opportunity to design, develop, and eventually implement a biocompatible magnesium material to be used for load-bearing endoprosthetic hip and knee implants. The favorable mechanical properties of Mg alloy include a high stiffness-to-mass ratio ( $(9 - 26) \times 10^6 \text{ m}^2 \cdot \text{s}^{-2}$ ) and, in particular, an elastic modulus (17 GPa in shear, 45 GPa in tension) in the range of that of cortical bone (7–30 GPa in tension). This suggests the eventual emergence of a novel biomaterial able to mitigate or even alleviate stress shielding [14] (see Section 5.2) caused by elastic property mismatch between implant and bone. Hence, effort is being expended on designing implant materials with a modulus that approaches that of bone. Ideally, the moduli of implant metal and bone should be identical (“isoelastic”) but this is an impossible task to date. Nevertheless, the exciting prospect of truly isoelastic endoprosthetic implants made from Mg alloy looms large on the horizon. Doubtless, there are still very substantial challenges to overcome. First among those is the need to improve the corrosion resistance of Mg base alloys by detecting novel biocompatible alloying elements as well as to discover appropriate biocompatible surface treatments that will guarantee long-term in vivo stability of the implant. Such surface treatments will include deposition of bioceramic coatings such as hydroxylapatite [15] and calcium silicates [16] as well as organosilanes [17] and polymeric hydrogels [18].

#### 4. Advantages of Hydroxylapatite Coatings

The advantages of osseoconductive hydroxylapatite coatings deposited on implant surfaces are manifold. Such coatings appear to reduce the time required for osseointegration of metallic implants and provide a genuine biochemically mediated strong bonding osteogenesis without a connective tissue capsule with gap formation that separate implant and cortical implant bed (see Figure 1A). In addition, they provide substantial corrosion resistance to the metallic parts of an implant and thus, efficiently counteract their corrosive deterioration.

A list of salient advantages includes [1]

- High biocompatibility
- High osseoconductivity
- Osseointegration in the presence of adsorbed bone growth-mediating proteins that result in faster and improved osseointegration
- No formation of fibrillar connective tissue surrounding the implant that separates it from the bone
- Osseointegration even in the presence of patient-induced micro-motion between implant and bone
- Formation of a strong bond between implant and bone with tensile strengths exceeding 35 MPa, depending on coating thickness
- Reliable reduction of pain after operation
- Earlier implant loading possible after healing phase
- Variable metallic substrates possible, including cp-titanium, titanium alloys, cobalt-chromium alloys, stainless steels, and magnesium alloys
- Variable surface structures possible, including mesh, artificial spongiosa, porous coatings, mechanically grooved surfaces, laser-patterned surfaces etc.
- Thickness of plasma-sprayed coatings can be selected between 50 and 250  $\mu\text{m}$ , depending on application; however, novel deposition techniques such as suspension or solution plasma spraying allow coatings with thickness  $<10 \mu\text{m}$ .
- Rarely problems with delamination and spalling in vivo
- Corrosion protection and hence, reduced or even completely alleviated release of potentially deleterious metallic ions to surrounding tissue
- In the presence of crystalline HAp, high dissolution/resorption resistance in contact with body fluid
- Quality control and standard according to ASTM F 1185-03 (2009) [19] designation

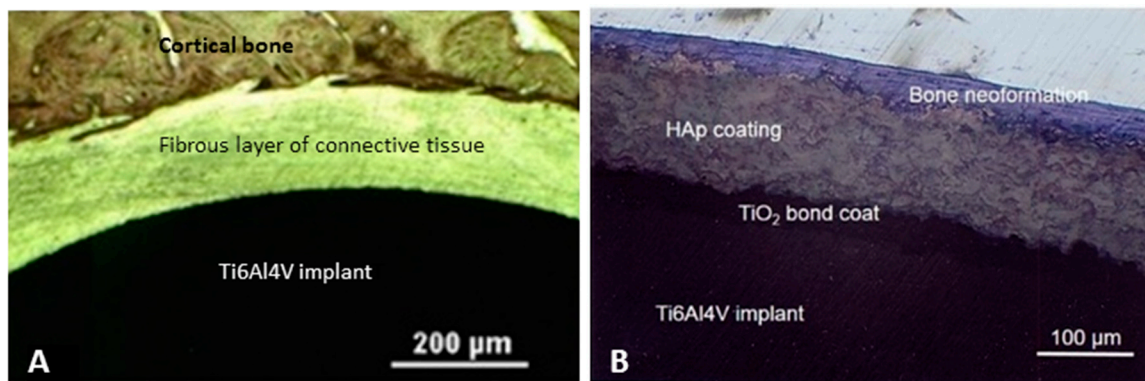


**Figure 1.** (A) Micrograph of a distal section of an uncoated Ti6Al4V rod implanted into the medulla of a sheep femur, showing the separation of the implant (black) and the bone (top) by a fibrous layer of connective tissue. (B) At the implant surface facing the marrow-filled femoral cavity, a thin bone lamella has formed adjacent to the continuous and intact hydroxylapatite (HAp) coating deposited by plasma spraying on a likewise plasma-sprayed TiO<sub>2</sub> bond coat. There is no formation of a connective tissue layer. Toluidine blue staining [20].

## 5. Sources of Implant Failure

### 5.1. Implant Failure by Interfacial Loosening

The relative level of reactivity of an implant influences the thickness of the interfacial layer between the biomaterial and the bone tissue. Bioinert ceramic implant materials such as alumina or zirconia but also cp-Ti and Ti alloys give rise to a non-adherent fibrous layer of connective tissue at the interface. If the implant is loaded such that interfacial micro-movement occurs, the normally very thin fibrous capsule can become several hundred micrometers thick (Figure 1A) and the implant loosens very quickly. In addition, to assure the biomechanical and biochemical functional performance of hip endoprostheses, particularly in elderly patients, the stem of the prosthesis will be solidly attached to the femoral bone by a biotolerant polymeric bone cement consisting of poly (methylmethacrylate) (PMMA). While this guarantees immediate fixation and early load-bearing capability, it is found to pose problems owing to the generation of elevated temperature during *in vivo* polymerization that may kill vital bone cells. In addition, production by abrasion of potentially carcinogenic polymer particles may occur that have been known to lead to osteolysis. These particles tend to migrate within the body through the lymphatic system causing the so-called “particle disease”. Particle disease is a (rare) lesion that results from an inflammatory response due to wear debris-induced osteolysis following arthroplasty. Particles resulting from the wear debris may cause macrophage activation and subsequent phagocytosis. Consequently, particle disease is often implicated to lead to aseptic joint loosening and concurrent implant failure.

To avoid catastrophic implant loosening, hydroxylapatite coatings on solid and porous Ti alloy implants were developed. The growth of bone into surface porosity provides a large interfacial area between the implant and its host, and thus, results in strong bonding osteogenesis, also called “biological fixation”. Most importantly, no formation occurs of a fibrous layer of connective tissue that would counteract solid implant fixation required for complete osseointegration (Figure 1B). This kind of fixation is capable of withstanding more complex stress states than those encountered in bioinert implants, most importantly tensile and shear stresses. In the case of porous implants, large pore sizes exceeding 75 μm (Table 1) are required for revascularization so that blood capillaries can provide a healthy blood supply to the ingrown connective tissue. When the porous implant is a metal, the large interfacial surface area may advance corrosion of the implant and loss of potentially toxic metal ions such as aluminum or vanadium to the surrounding tissue. Hence, coating a porous metal implant with a bioactive ceramic, such as hydroxylapatite, can reduce or even annihilate corrosion. The bioactive

(osseointegrative) coating also enhances the rate of bone growth into the pores. However, the coatings often dissolve with time and thus, limit their effectiveness. Degradation of coatings may also produce particles that are able to migrate through the body and give rise to the “particle disease” mentioned above. Since the large size and volume fraction of porosity required for stable interfacial bone growth degrades the strength of the material, the porous method limits its application to coatings or unloaded space fillers in tissues.

Moreover, other potentially deleterious biological interventions may lead to premature implant loosening. For example, if by some metabolic processes, e.g., inflammation in response to infection with *staphylococci* the pH of body fluid will decrease to below 4.5, hydroxylapatite will start to dissolve (see below). This has severe consequences for the stability of implants carrying HAp coatings, as it will promote loosening of the endoprosthesis.

### 5.2. Implant Failure by Stress Shielding

A general mechanical problem is manifest at the interface between a biomaterial implant and bone: stress shielding caused by elasticity mismatch between implant and bone. Since the biomaterial has inevitably a much higher modulus of elasticity compared to both cortical and cancellous bone (Figure 2), the implant carries almost the entire load during ambulatory movement. However, since bone must always be loaded in tension to remain healthy, the lack of load or insufficient loading results in bone atrophy, i.e., weakening of the bone in areas that are either unloaded or weakly loaded in tension or loaded in compression. Hence, effort is being spent on designing implant materials with a modulus that approaches that of bone. Ideally, the moduli of biomaterials and bone should be identical (“isoelastic”) but this is an impossible option to date. As shown in Figure 2, extremely stiff materials such as alumina, CoCrMo alloy, or A/W glass ceramic have elastic moduli much higher than those of cortical and cancellous bone, respectively. However, Ti alloys, bioglass, novel biocomposites, and in particular Mg alloys show moduli much closer to that of bone. Indeed, elimination of stress shielding is a primary motivation to design biocomposites with elastic moduli matching those of bone. Such novel isoelastic biocomposites will provide a two-prong approach: enhanced biocompatibility as expressed by its osseointegrative properties, and enhanced mechanical, i.e., elastic compatibility with the host bone. It is suggested that novel, corrosion-resistant Mg alloys are destined to be part of a new generation of biomaterials that possess such favorable mechanical, chemical, and biological properties.

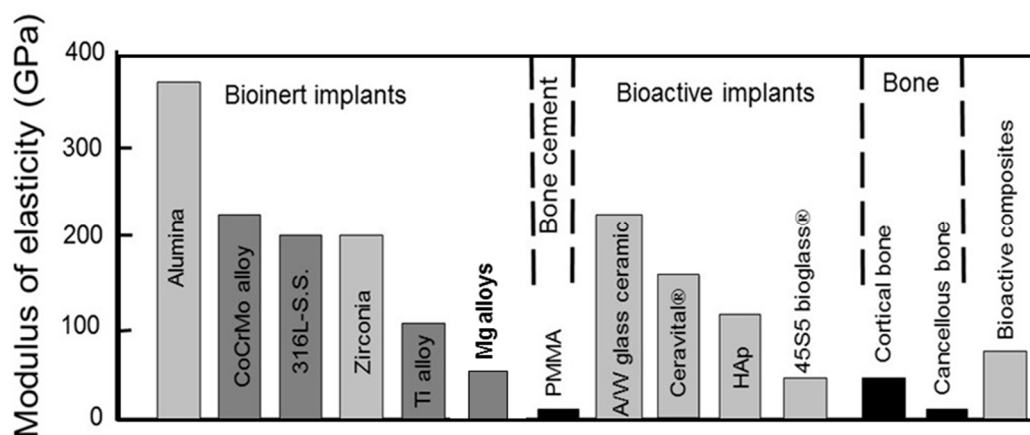


**Figure 2.** Moduli of elasticity of prosthetic biomaterials in comparison to cortical and cancellous bone. Light grey: ceramics, dark grey: metals, black: polymers.

## 6. Coating Deposition by Plasma Spraying

Deposition of hydroxylapatite coatings onto the stems of commercial hip endoprostheses and parts of dental root implants is most frequently been done by atmospheric (air) plasma spraying.

Plasma spraying is a coating technology during which material, either as a solid, suspension or a liquid, is introduced into a plasma jet and is propelled with high velocity against the surface to be coated. The technology is versatile since any thermally reasonably stable metallic, ceramic or even polymeric material with a well-defined melting point can be coated onto nearly any surface. However, in praxis many limitations persist that may result in high coating porosity, insufficient adhesion to the substrate, and deleterious residual coating stresses. In addition, plasma spraying, as a line-of-sight technology, inhibits deposition of coatings on geometrically complex surfaces or surfaces with high inner porosity.

The mode of injection of powder particles into the plasma jet depends on the grain size, the melting temperature, and the thermal stability of the powder material. In general, injection can be perpendicular to the jet at the point of exit of the jet from the anode nozzle of the plasma torch, in upstream or downstream mode at an angle to the jet axis, directly into the nozzle, or coaxially through a bore in the cathode. Upstream injection is used when increased dwell time of the powder particles in the jet is required, i.e., when spraying high refractory materials. Downstream injection protects a powder with a low melting point from decomposition and vaporization, respectively. This mode is frequently used when spraying hydroxylapatite.

The plasma jet is formed by ionization in an electric potential field of a suitable gas, preferentially argon, nitrogen or even helium. To increase the thermal conductivity of the plasma gas and thus, the heat transfer from plasma to the material to be sprayed, frequently an auxiliary gas such as hydrogen is added. The resulting plasma consists of positively charged ions and electrons but also neutral gas atoms and photons. Moving charges within the plasma column induce a magnetic field  $B$  perpendicular to the direction of the electric field, characterized by the current  $j$ . The vector cross product of the current,  $[j \times B]$  is the magneto-hydrodynamic Lorentz force, the vector of which is mutually perpendicular to  $j$  and  $B$ . Hence, an inward moving force is created that constricts the plasma jet by the so-called magnetic or z-pinch. In addition to this magnetic pinch, there is a thermal pinch that results from reduction of the thermal conductivity of the plasma gas at the cooled inner wall of the anode nozzle, leading to an increase in current density at the center of the jet. Hence, the charged plasma tends to concentrate along the central axis of the plasma torch thereby confining the jet. As the result of these two effects, the pressure in the plasma core increases drastically and hence, the jet is blown out of the anode nozzle with supersonic velocity.

A portion of this supersonic velocity will be transferred to the injected powder particles, i.e., the powder particles will gain acceleration from the plasma jet by momentum transfer. The particle acceleration  $dV_p/dt$  is proportional to the drag coefficient  $C_D$  and the velocity gradient between the gas velocity  $V_g$  and the particle velocity  $V_p$ , and inversely proportional to the particle diameter  $d_p$  and the particle density  $\rho_p$  as expressed by the Basset-Boussinesq-Oseen (BBO) equation of motion,

$$\frac{dV_p}{dt} = \left[ \frac{3C_D \cdot \rho_g}{4d_p \cdot \rho_p} \right] \cdot (V_g - V_p) \cdot |V_g - V_p| \quad (1)$$

A large part of the (electric) energy spent on ionization of the plasma gas will be recovered by recombination in the form of heat, and hence, the powder particles accelerated by momentum transfer along a trajectory in the jet will be heated by the hot plasma. The amount of heat a particle acquires can be approximated by the balance of the amounts of heat gained by convective energy transfer,  $Q_C = h \cdot A \cdot (T_\infty - T_s)$  and of heat lost by radiative energy transfer,  $Q_R = \sigma \cdot \varepsilon \cdot A \cdot (T_s^4 - T_a^4)$  with  $h$  = convective heat transfer coefficient,  $A$  = surface area of the particle,  $T_\infty$  = free-stream plasma temperature,  $T_s$  = particle surface temperature,  $T_a$  = temperature of the surrounding atmosphere,  $\sigma$  = Stefan-Boltzmann coefficient, and  $\varepsilon$  = particle emissivity. The heat transfer coefficient between a fluid and a (spherical) particle is frequently expressed by the Ranz-Marshall equation as a function of the non-dimensional Nusselt number, Nu:

$$\text{Nu} = 2.0 + b \cdot \text{Re}^m \cdot \text{Pr}^n \quad (2)$$

where  $Re$  = Reynolds number and  $Pr$  = Prandtl number.

The powder particles melted in the hot plasma jet will impact the surface to be coated with high velocity and splash as depicted in Figure 3A which shows the surface of a plasma-sprayed hydroxylapatite coating with typical overlapping, pancake-shaped particle splats as well as some incompletely melted (oversized) particles that cling loosely to the surface. In the cross-section, there is evidence of an amorphous calcium phosphate layer immediately adjacent to the substrate and a titania bond coat, respectively (Figure 3B). This ACP layer forms a low energy fracture path along which the coating may delaminate from the metal substrate in the presence of shear stresses [21].

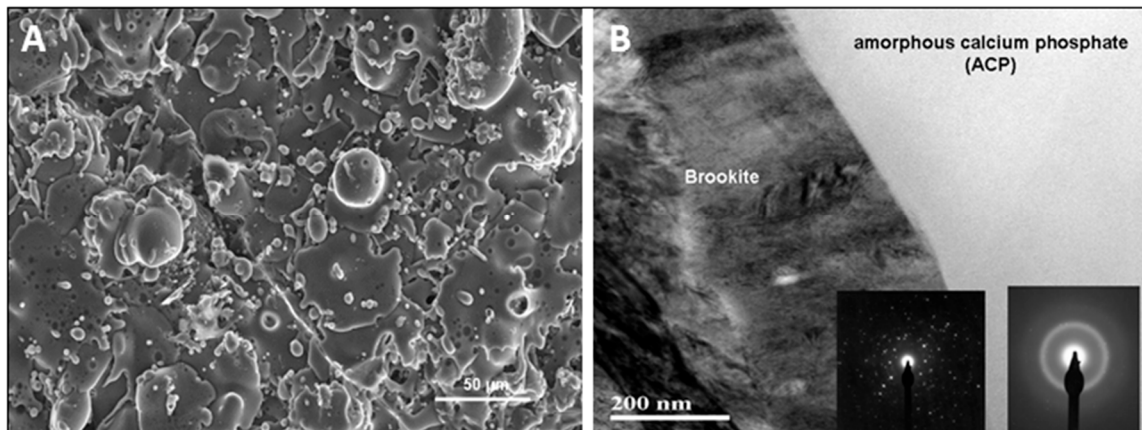


**Figure 3.** (A) Characteristic surface features of a typical plasma-sprayed hydroxylapatite coating with overlapping pancake-like particle splats and some loosely adhering incompletely melted particles [1]. (B) Bright field STEM image of a cross-section of a plasma-sprayed hydroxylapatite coating on Ti6Al4V. Shown is the interface between an oriented polycrystalline titania (brookite) bond coat (left) and an amorphous calcium phosphate (ACP) top coat (right). The insets show electron diffraction pattern of both phases [22].

Selection of appropriate intrinsic (plasma power, argon gas flow rate, auxiliary gas flow rate, powder carrier gas flow rate etc.) and extrinsic (spray distance, powder feed rate, powder grain size, particle morphology, surface roughness etc.) plasma spray parameters is crucial for sufficient powder particle heating, flow and surface wetting on impact. Hence, painstaking selection of these parameters leads to development of the desired coating porosity and adhesion to the substrate. Of particular importance are the powder flow characteristics that must be carefully engineered to yield an uninterrupted and strictly controlled powder feed rate to the plasma torch. In addition, the electrical power level of the plasma torch must be selected in such a way as to avoid overheating of powder particles. Overheating might lead to an “exploded” splat configuration with increased microporosity, depleted and evaporated material, as well as high residual stresses and, consequently, reduced adhesion strength of the coatings.

It is a fact well known to practitioners of plasma spraying that the properties can vary widely from coating to coating even though the spray parameters have supposedly been set within narrow ranges using sophisticated microprocessor-controlled metering devices and stringent quality control measures including statistical process control (SPC), Taguchi methodology, and the like. This inability to exactly reproduce mechanical, chemical, tribological, and biological properties of APS coatings has serious consequences in terms of establishing clinical performance and quality control protocols. The reason for this is deeply rooted in the non-linear nature of the deposition process. More details on the physics and technology of the plasma-spraying process and, in particular, plasma spraying of hydroxylapatite can be found in several textbooks written by the author [1,23,24].

## 7. Key Characteristics of Plasma-Sprayed Hydroxylapatite Coatings

Osseoconductive ceramics such as hydroxylapatite show a positive interaction with living tissue including chemical bonding to the bone along the interface, triggered by the adsorption of bone growth-mediating proteins at the biomaterials surface. Such osseostimulating cytokines include the transforming growth factor  $\beta$  (TGF- $\beta$ ), insulin-like growth factor (IGF-1), and in particular the family of rhBMPs (recombinant human bone morphogenetic proteins). Hence, owing to the presence of these cytokines, there will be a biochemically-mediated strong bonding osteogenesis triggered by the process of osseointegration [25–27]. In addition to compressive forces, to some degree tensile and shear forces can also be transmitted through the interface (“bony in-growth”). Typical osseoconductive materials such as calcium phosphates [28] and bioglasses [29,30] become osseointegrative by adsorption of bone-growth stimulating proteins. The term osseointegrativity refers to the transformation of undifferentiated mesenchymal stem cells into osseoprogenitor cells that eventually form osteoblasts, i.e., mononucleated bone cells.

Among calcium phosphates, hydroxylapatite takes on a dominating role in bioengineering. Hydroxylapatite is one of the most important and consequently most researched bioceramic materials. Biological apatite that forms the inorganic scaffolding materials of bone is chemically and structurally very close to naturally occurring geologic hydroxylapatite. However, bioapatite differs from inorganic hydroxylapatite in several important aspects. They include exceptionally small grain size in the nanometer range, high degree of carbonate substitution for phosphate and hydroxyl ions, noticeable OH deficiency, partial replacement of Ca ions by other metabolically important elements, presence of lattice vacancies, and increased solubility that is responsible for bone remodeling in response to varying stress levels. Moreover, hydroxylapatite as a synthetic ceramic material is mechanically weak and hence, unable to sustain even moderate tensile, shear, or compressive forces. Consequently, it cannot be applied as monolithic material per se such as the structurally strong bioinert ceramics alumina or zirconia. Instead, it is applied either in granular form to fill larger bone cavities or, most frequently, as coatings for metallic implants to lend osseointegrative and, in conjunction with adsorbed bone growth-mediating proteins, osteointegrative properties to the bioinert or biotolerant metallic implant surface as described above.

For a general account on material properties of hydroxylapatite, see Willmann [31]. Callahan et al. [32], and Wintermantel and Ha [33] have suggested guidelines for the performance profile of plasma-sprayed hydroxylapatite coatings (Table 1). A recent review paper by Demnati et al. [34] highlights the salient physico-chemical features and the influence they have on biological consequences and in vivo performance.

Apart from the need of biocompatibility to support bone ingrowth by providing attachment sites for bone growth-mediating proteins, osseointegrative hydroxylapatite coatings must possess properties that positively influence their performance in vivo. These properties include optimum adhesion strength, stable phase composition, phase purity, sufficiently high crystallinity, adequate porosity, surface roughness and microtopography, reduced deleterious residual coating stresses, suitable thickness, as well as provision of sufficient corrosion protection to the metallic substrate.

### 7.1. Adhesion Strength

In contrast to a desired value of at least 35 MPa (Table 1), the adhesion strength of plasma-sprayed hydroxylapatite layers to a titanium alloy implant surface was found to be notoriously weak. Adhesion is overwhelmingly provided by mechanical clamping of coating particles to asperities of the roughened surface of the metallic substrate. Despite claims that a thin reaction layer of calcium dititanate ( $\text{CaTi}_2\text{O}_5$ ) or calcium titanate (perovskite,  $\text{CaTiO}_3$ ) exists that will mediate adhesion [35–37], experimental evidence of such a reaction layer in as-sprayed coatings is scant or absent. Owing to its thinness, visualization by transmission electron microscopy even at high magnification [20] is hampered by its exiguity owing to the very short diffusion paths of  $\text{Ca}^{2+}$  and  $\text{Ti}^{4+}$  ions, respectively, that render any potential reaction zone extremely thin.

To improve adhesion, the degree of melting of the HAp particles in the plasma jet ought to be improved by an increase of the plasma enthalpy. However, there is a conflict: high plasma enthalpies inevitably lead to increased thermal decomposition of the incongruently melting hydroxylapatite and thus to a decrease of its resorption resistance, i.e., the *in vivo* longevity of the coatings. Consequently, the intrinsic and extrinsic plasma spray parameters and the resulting microstructure of the deposited coatings need to be carefully optimized by controlling the heat transfer rate from the hot core of the plasma jet to the center of the powder particles [23]. Alternatively, other solutions have been sought that include addition of suitable bond coats mediating the adhesion of the coatings [1,38], microstructural patterning of the substrate surface by etching or laser treatment, as well as functional gradient coatings with reduced residual stress states [39].

**Table 1.** Property profile of plasma-sprayed hydroxylapatite (HAp) coatings [32,33].

Property	Dimension	Reference [32]	Reference [33]	Function
Adhesion Strength	MPa		>35	Implant Integration
HAp Content	%	>95	>95	Chemical Stability
Purity	ppm	<50		Biocompatibility
Crystallinity	%	>62	>90	Resorption Resistance
Roughness	μm		>75	Optimum Cell Ingrowth
Porosity	%	Determined by ASTM F1854 [40]		Revascularization
Coating Thickness	μm		<50	Easy Resorption
			50 < x < 200	Long-Term Stability
Tensile Strength	MPa	>51		Coating Integrity
Shear Strength	MPa	>22		In Vivo Adhesion Strength

Considerable research has been expended on improving the adhesion of hydroxylapatite coatings to metallic substrates by applying appropriate bond coats. An ideal bond coat should have several characteristics that include uncompromised biocompatibility, good adhesion to both the metal substrate and the osseoconductive top coat, and a well-defined melting point to allow application of thermal spray technology. In addition to the adhesion-mediating function, suitable bond coats ought to have the following properties:

- The bond coat should prevent direct contact between Ti and HAp since metallic Ti has the potential to catalyze thermal decomposition of HAp.
- The bond coat should reduce or even completely prevent the release of potentially cytotoxic metal ions from a corroding metallic substrate to the surrounding living tissue.
- The bond coat should reduce the thermal gradient at the substrate/coating interface induced by the rapid quenching of the molten particle splats. This fast quenching leads to deposition of amorphous calcium phosphate (ACP) with an associated decrease in resorption resistance and hence reduced *in vivo* performance, i.e., reduced longevity of the implants.
- The bond coat should prevent a steep gradient in the coefficients of thermal expansion between substrate and coating that will otherwise induce large residual tensile stresses leading to cracking and delamination of the coatings.
- The bond coat should cushion damage to the coating initiated by cyclic micromotions of the implant during movement of the patient in the initial phase of osseointegration.

Numerous types of bond coat [38] were experimentally applied including calcium silicates [41], titania [42] (see Figure 3B), and zirconia [39].

### 7.2. Phase Composition and Degree of Crystallinity

These coating properties are of vital importance for coating in-service performance as they control crucially the *in vivo* dissolution behavior. Highly crystalline and thus stoichiometric HAp is only sparingly soluble at pH values above 4.5, showing essentially bioinert characteristics and an inhibiting

effect on cell differentiation, as confirmed by decreased levels of alkaline phosphatase (ALP) activity and osteocalcin secretion. In contrast, amorphous calcium phosphate (ACP), thermal decomposition products of hydroxylapatite such as tricalcium phosphate (TCP), tetracalcium phosphate (TTCP) and calcium oxide (CaO), as well as dehydroxylation products with short-range order (SRO) structure such as oxyhydroxylapatite (OHAp) and/or oxyapatite (OAp) show enhanced solubility in human blood serum and simulated body fluid (SBF) [43].

During plasma spraying, hydroxylapatite particles undergo thermal dehydroxylation to form oxyhydroxylapatite and oxyapatite [44] and, eventually, thermal decomposition forming tri- and tetracalcium phosphates according to the stepwise sequence of events as shown in Table 2.

**Table 2.** Thermal decomposition sequence of plasma-sprayed hydroxylapatite.

Step 1	$\text{Ca}_{10}(\text{PO}_4)_6(\text{OH})_2$ Hydroxylapatite	→	$\text{Ca}_{10}(\text{PO}_4)_6(\text{OH})_{2-2x}\text{O}_x\text{□}_x + x\text{H}_2\text{O}$ Oxyhydroxylapatite
Step 2	$\text{Ca}_{10}(\text{PO}_4)_6(\text{OH})_{2-2x}\text{O}_x\text{□}_x$ oxyhydroxylapatite	→	$\text{Ca}_{10}(\text{PO}_4)_6\text{O}_x\text{□}_x + (1-x)\text{H}_2\text{O}$ oxyapatite
Step 3	$\text{Ca}_{10}(\text{PO}_4)_6\text{O}_x\text{□}_x$ oxyapatite	→	$2\text{Ca}_3(\text{PO}_4)_2 + \text{Ca}_4\text{O}(\text{PO}_4)_2$ tricalcium phosphate + tetracalcium phosphate
Step 4a	$\text{Ca}_3(\text{PO}_4)_2$ tricalcium phosphate	→	$3\text{CaO} + \text{P}_2\text{O}_5 \uparrow$
Step 4b	$\text{Ca}_4\text{O}(\text{PO}_4)_2$ tetracalcium phosphate	→	$4\text{CaO} + \text{P}_2\text{O}_5 \uparrow$

On contact with simulated body fluid (SBF) or biofluid, parts of the hydroxylapatite-based coating dissolve according to the sequence of solubility shown in Equation (3) and Figure 4.

Figure 4 shows the pH dependence of solubility isotherms of several biologically important calcium phosphate phases. From this diagram, the following order of solubility results [45]:

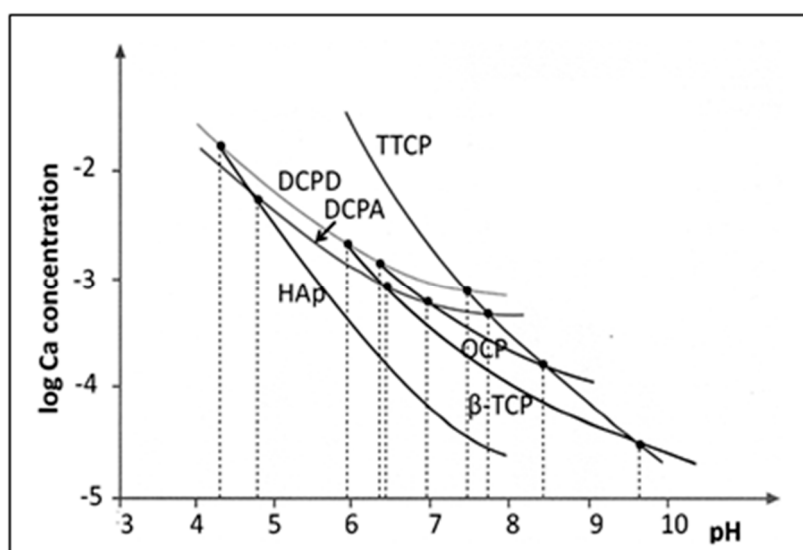


**Figure 4.** Solubility isotherms of calcium phosphates at 25 °C. HAp: hydroxylapatite, DCPD: brushite, DCPA: monetite,  $\beta$ -TCP:  $\beta$ -tricalcium phosphate, OCP: octacalcium phosphate, TTCP: tetracalcium phosphate [1]. © With permission by Wiley-VCH.

Moderately enhanced levels of  $\text{Ca}^{2+}$  and  $\text{HPO}_4^{2-}$  ions in the biofluid adjacent to the interface implant-tissue are desired as they assist bone remodeling. However, excessive amounts of these ions released from the dissolving decomposition products of plasma-sprayed HAp are known to drive up the local pH value with concurrent cytotoxic effects on living bone cells. Consequently, short-term release of ions from dissolving calcium phosphate phases must be kept at bay and, in fact, minimized by increasing the amount of well-crystallized HAp in the as-sprayed coatings [46].

Interaction of plasma-sprayed hydroxylapatite coatings with simulated body fluid (SBF) in vitro or biofluid in vivo tends to dissolve easily soluble components such as CaO, tetracalcium phosphate (TTCP), and amorphous calcium phosphate (ACP). Table 3 shows an increase in HAp from  $71.8 \pm 1.7\%$  in the as-sprayed coating ( $t = 0$ ) to  $82.8 \pm 2.3\%$  after incubation in r-SBF [47] for 56 days whereas the amount of TTCP decreased from  $23.6 \pm 1.6\%$  ( $t = 0$ ) to  $9.1 \pm 1.9\%$  ( $t = 56$ ). During the same period, the amount of cytotoxic CaO decreased from  $1.3 \pm 0.3\%$  to zero.

**Table 3.** Phase content of plasma-sprayed and incubated hydroxylapatite coatings as obtained by Rietveld refinement [1,48].  $t$  incubation time,  $\sigma$  standard deviation (95% confidence level), HAp hydroxylapatite, TTCP tetracalcium phosphate,  $\beta$ -TCP  $\beta$ -tricalcium phosphate.

$t$ (Days)	HAp (%)	$\sigma$ (%)	TTCP (%)	$\sigma$ (%)	$\beta$ -TCP (%)	$\sigma$ (%)	CaO (%)	$\sigma$ (%)	CaCO <sub>3</sub> (%)	$\sigma$ (%)
0	71.8	1.7	23.6	1.6	3.3	1.1	1.3	0.3	-	-
1	72.5	1.5	23.5	1.4	3.2	1.0	0.7	0.2	-	-
7	70.9	2.3	21.8	2.1	4.5	1.3	0.4	0.3	2.5	0.8
28	70.6	1.9	22.0	2.0	6.2	1.4	-	-	1.2	0.9
56	82.8	2.3	9.1	1.9	6.2	1.6	-	-	1.9	0.7

### 7.3. Porosity and Surface Roughness

Besides adhesion, phase composition, and crystallinity of the coatings, their porosity as well as their surface roughness play decisive roles in the quest for enhancing the biomedical performance of endoprosthetic implants. Whereas optimum coating porosity and roughness (Table 1) are mandatory for the ingrowth of bone cells and subsequent revascularization, accumulation during plasma spraying of macropores at the substrate/coating interface leads to an intolerable weakening of the coating adhesion as well as cohesion. The denser the microstructure of the bioceramic coating, the lower is the risk of bonding degradation by cracking, spalling, and delamination during in vivo contact with aggressive body fluids. However, since the integrity and continuity of the substrate/coating interface is of paramount importance for implants, the two conflicting requirements of the need of porosity for bone cell ingrowth and the need of high coating density for superior adhesion have to be carefully balanced and controlled [48]. This is particularly important when considering the risk of release of coating particles that will be distributed by the lymphatic system and is known to lead to inflammatory responses (“particle disease”) with formation of undesirable giant cells and phagocytes. Hence, balancing the two conflicting porosity requirements is a considerable challenge during designing and controlling appropriate intrinsic plasma spraying parameters.

In addition to coating porosity, adequate surface nanotopography is a prerequisite for optimum cell adhesion and proliferation [49]. Recently, the extent of surface topography has been successfully described by the concept of fractality. Fundamental experiments were conducted to study cell proliferation on electrochemically etched silicon proxy surfaces with varying roughness but comparable surface free energies. The surface profile was found to be a self-affine fractal [50], the average roughness  $R_a$  of which increases with etching time from  $\sim 2$  nm to 100 nm, with fractal dimension ranging from 2 (a nominal flat surface) to 2.6. A moderately rough surface with  $R_a$  between 10 and 45 nm yields a close to Brownian surface with  $D \sim 2.5$  [51]. The authors of this study [49] concluded that the observed cell behavior could be satisfactorily explained by the theory of adhesion to randomly rough solids, and that a moderately rough surface with large fractal dimension is conducive to proliferation, suitable

spreading, and vitality of bone cells. Gittens et al. [52] have recently reviewed and interpreted the influence of surface topography including micro-roughness and nanostructures on the osseointegration of spinal implants.

#### 7.4. Residual Stresses

The occurrence of residual stresses at the interface hydroxylapatite coating-metallic implant as well as within the coating will result in reduced adhesion by the occurrence of delamination and crack formation, depending on the magnitude and sign of the stresses. Residual stresses originate from the large temperature gradients experienced during the plasma spraying process. When the molten particles strike the cold substrate, they are rapidly quenched whereby their contraction is constrained by tight adherence to the rough and rigid substrate. This leads to accumulation of high levels of tensile stresses both within the coating and at the coating-to-substrate interface, commonly referred to as “quenching stresses” [53]. The first layer adjacent to the interface, found to consist of amorphous calcium phosphate (ACP) [18] (see Figure 3B), will crucially control the occurrence of residual stresses in terms of magnitude as well as sign. In addition, this thin layer provides a low-energy fracture path that may lead to coating delamination in the presence of tensile residual stresses [21]. However, the transformation of ACP to crystalline calcium phosphate phases during in vitro contact with simulated body fluid and in vivo contact with biofluid, respectively will lead to stress relaxation as observed by Heimann et al. [54] and Topić et al. [53], and thus, reduces the risk of coating failure by delamination.

Figure 5 shows the lattice strain of hydroxylapatite coatings deposited by plasma spraying on Ti6Al4V substrates measured as a function of  $\sin^2\psi$ , where  $\psi$  is the tilt angle towards the X-ray beam. The as-sprayed coatings exhibit rather strong compressive surface stresses owing to thermal mismatch developed during cooling of the deposited layer to room temperature. This compressive stress relaxes during incubation in simulated body fluid when amorphous calcium phosphate (ACP), thought to be a main contributor to the residual stress, crystallizes to form calcium phosphate phases, most notably TTCP and HAp. Hence, the layer of bone-like secondary apatite deposited at the outermost rim of the samples is decoupled from the declining stress field, and thus, shows close to zero stress as evident from Figure 5.

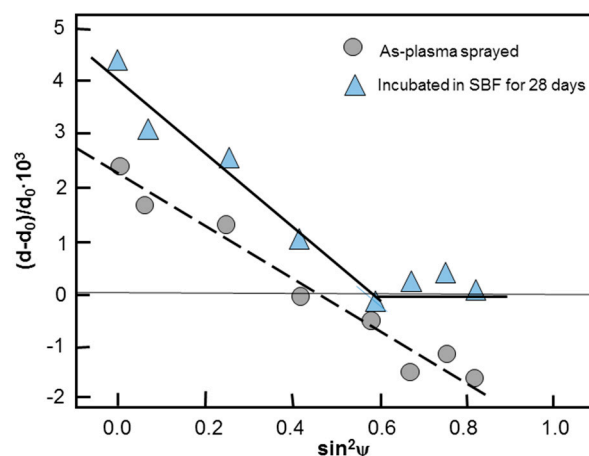


**Figure 5.** Development of near-surface residual stresses in as-sprayed HAp coatings (dotted line) and coatings incubated in simulated body fluid (SBF) for 28 days (solid line) [54].

Whereas during deposition the substrate is usually at some elevated temperature, post-depositional cooling to room temperature generates additional stress by thermal mismatch proportional to the differences in the thermal expansion coefficients of the coating and the substrate as well as the intrinsic elastic moduli. The principal equation governing the generation of thermal

coating stress  $\sigma_c$  was derived by the German glass chemist Adolf H. Dietzel and can be expressed by the equation,

$$\sigma_c = \frac{\{E_c(\alpha_c - \alpha_s) \cdot \Delta T\}}{1 - \nu_c} + \left[ \frac{1 - \nu_s}{E_s} \right] d_c/d_s \quad (4)$$

where  $E$  = Young's modulus,  $\alpha$  = coefficient of thermal expansion,  $T$  = temperature,  $\nu$  = Poisson's number, and  $d$  = thickness. The subscripts  $c$  and  $s$  refer to coating and substrate, respectively. Since at given values of  $\nu$  and  $E$  the thermal coating stress  $\sigma_c$  increases with increasing coating thickness  $d_c$ , the risk of spalling is much higher in thick coatings than in thin ones. Moreover, depending on the sign of  $(\alpha_c - \alpha_s)$ , the so-called "thermal stress" can either be tensile or compressive. Quenching and thermal stresses, combined with the complicated solidification process of the coating, are the two main contributors to the overall residual stress. Hence, control of residual stresses is important for the integrity of the coating-substrate system and in turn, its mechanical performance since high residual stresses can lead to cracking and delamination of the coating, shape changes of thin substrates, and in general can undermine the performance of the entire part. Tensile stresses exceeding the elastic limit of the coating, cause cracking perpendicular to the direction of the tensile stress tensor. Whereas in general some degree of compressive stress is considered desirable as it closes cracks originating at the surface and thus improves fatigue and corrosion properties, excessive compressive stress can cause adhesive failure as shown in Figure 6.

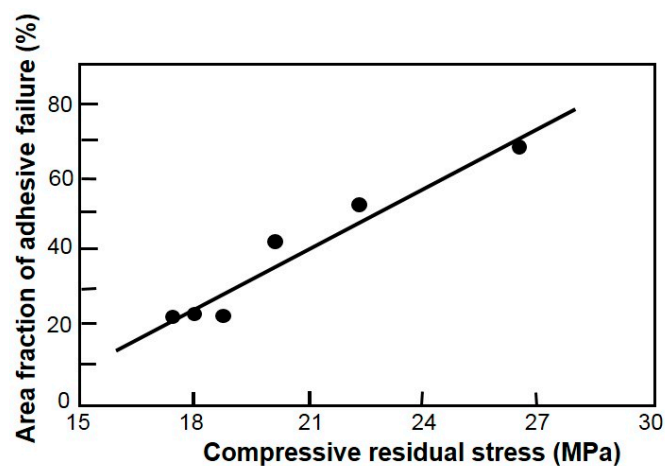


**Figure 6.** Relation between adhesive failure and compressive residual stresses of plasma-sprayed hydroxylapatite coatings on Ti6Al4V [55]. © With permission by Elsevier.

In biomedical service, the existing residual stresses superpose with the applied loading stress during movement of the patient and failure may occur or fatigue life be shortened if the residual stress is sufficiently high. Hence, stringent control of the occurrence of high residual stresses is of paramount importance in the quest for optimum mechanical coating performance.

### 7.5. Coating Thickness

It is well known that a thin HAP layer (<50  $\mu\text{m}$ ) yields better adhesion strength compared with thicker coatings (Table 1) on account of reduced residual coating stress (see Equation (4)). However, residual stresses will be quickly relaxed in the course of bone integration. Even though thicker coatings ( $\pm 150 \mu\text{m}$ ) show substantially reduced adhesion strength, they may be required in some instances to ensure a more permanent bond to guarantee implant stability by a lasting biological effect [18,56,57]. This is particularly evident when during an endoprosthetic replacement operation involving a corrective exchange of the implant the cortical bone matter has been previously damaged, often in concurrence with an undesirable geometric configuration of the implant-supporting cortical bone. In this special case, a thin, rapidly resorbed calcium phosphate coating will not be sufficient to

sustain the required large-scale bone regeneration. Hence, thicker coatings will be required to stimulate bone reconstruction over longer times.

### 7.6. Corrosion Protection

Hydroxylapatite coatings are supposed to assist in preventing the release of metal ions from the metallic implant to the surrounding living tissue. Heavy metal ions have been found to cause hepatic and renal degeneration in animals [58] as well as impaired development of human osteoblasts. There are, however, reports that V-containing implants may reduce osteoclast (OC) activity at the bone-implant interface and thereby decrease bone resorption and ultimately the rate of implant failure [59]. In contrast, heavy metal ions, in particular vanadium possibly released from Ti6Al4V alloy, are thought to affect negatively the transcription of DNA to RNA in cell nuclei and, in addition, influence the activity of enzymes by replacing Ca or Mg ions at binding sites. Hence, the metabolic action of aluminum and vanadium ions released from the implant and their interference with normal biochemical functions of the human body are an important intervention to consider and require more study [60]. Consequently, today, developments are on the way to replace Ti6Al4V by low modulus ( $E < 50$  GPa)  $\beta$ -type Zr-containing alloys such as Ti13Nb13Zr free of potentially deleterious Al and V.

Whereas corrosion protection of Mg alloys is predominantly based on conversion coatings consisting of MgO, Mg(OH)<sub>2</sub> or MgF<sub>2</sub>, hydroxylapatite coatings deposited by biomimetic or other low temperature deposition techniques have been shown to reduce substantially the corrosion rate of magnesium [15].

Potentiodynamic polarization testing [61] is frequently being used to characterize the ability of bioceramic coatings to provide corrosion protection to the metal implant substrate underneath. Figure 7A shows potential vs. current density plots of uncoated bioinert Ti6Al4V (1), Ti6Al4V coated with sol-gel-derived hydroxylapatite (2), and Ti6Al4V dip-coated with a homogeneous crack-free poly( $\epsilon$ -caprolactone)/hydroxyapatite composite coating (3; 30% PCL/70% HAp). The current densities decreased substantially from  $2.7 \times 10^{-7}$  (curve 1) to  $6.2 \times 10^{-8}$  (curve 2) to  $7.7 \times 10^{-9}$  A·cm<sup>-2</sup> (curve 3). It ought to be noted that the presence of polymer provided additional protection by sealing pores in the hydroxylapatite coating. The corrosion potentials  $E_{\text{corr}}$  were found to increase from  $-0.37$  V (curve 1) to  $-0.23$  (curve 2) to  $-0.08$  V (curve 3). Concurrently, the polarization resistance  $R_p$  increased from  $9.1 \times 10^5$   $\Omega$ ·cm<sup>2</sup> (curve 1) to  $7.0 \times 10^6$   $\Omega$ ·cm<sup>2</sup> (curve 2) to  $1.5 \times 10^7$   $\Omega$ ·cm<sup>2</sup> (curve 3).

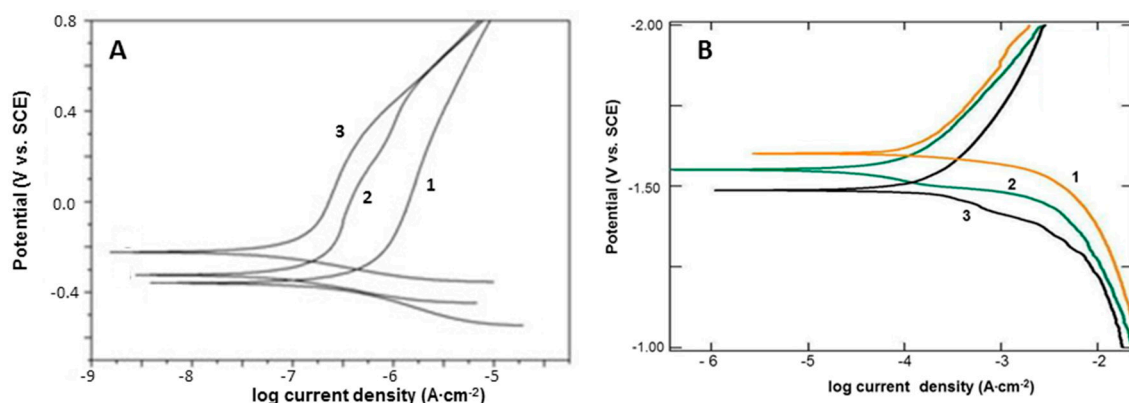


**Figure 7.** (A) Potentiodynamic polarization curves of uncoated Ti6Al4V alloy (1), Ti6Al4V sol-gel coated with hydroxylapatite (2), and Ti6Al4V dip-coated with a hydroxylapatite/poly( $\epsilon$ -caprolactone) composite coating (3). (B) Potentiodynamic polarization curves of uncoated biodegradable WE43 Mg alloy (1), WE43 Mg alloy electrophoretically (2), and pulsed laser deposition (3) coated with hydroxylapatite [62]. For explanation, see text. © With permission by Elsevier.

Figure 7B shows a typical example of potential vs. current density plots of biodegradable medium-entropy WE43 Mg alloy (1), WE43 Mg alloy electrophoretically (EPD) coated with

hydroxylapatite (2), and WE43 Mg alloy pulsed laser-deposited (PLD) with hydroxylapatite (3) [62]. The two types of coating improved the electrochemical stability of the substrate metal as ascertained by shifting the polarization curves towards lower corrosion current densities, from  $1.9 \times 10^{-4}$  (curve 1) to  $9.0 \times 10^{-5}$  (curve 2) to  $2.5 \times 10^{-5} \text{ A}\cdot\text{cm}^{-2}$  (curve 3), corresponding to corrosion rates decreasing from 0.97 to 0.19 to 0.07 mm/year, respectively. Concurrent with this improved corrosion resistance, the corrosion potentials  $E_{\text{corr}}$  were found to increase from  $-1.60 \text{ V}$  for uncoated Mg alloy to  $-1.55 \text{ V}$  for EPD-HAp coatings to  $-1.49 \text{ V}$  for PLD-HAp coatings.

Evaluation of the potential-current density curves shown in Figure 7 is done by applying Tafel theory [63]. This theory stipulates that the rates of anodic and cathodic partial reactions become equal at the corrosion potential  $E_{\text{corr}}$ , at the intersection of the tangents to the anodic and cathodic branches of the potential-current density curve. Consequently, the electrochemical parameters of most metals can be obtained from the so-called Tafel slopes of a potential-current density plot provided by potentiodynamic polarization (PDP) experiments.

## 8. A Novel Class of Bioceramics: Transition Metal-Substituted Calcium Phosphates

Calcium (Ti,Zr) hexaorthophosphates with NaSiCON structure constitute a novel class of bioceramic materials that, based on their favorable chemical, electrical, and biomedical properties, promise successful application to accelerate bony integration of endoprosthetic implant devices and to speed up healing of broken bones [1,20,64–66]. A novel device has been proposed [67] for this purpose, the advantage of which, over already existing bone-growth stimulators, is its ability to provide the intimate contact of a capacitive-coupled electric field with the growing bone tissue as opposed to an externally applied inductively coupled electromagnetic field. As this field suffers substantial attenuation when transmitted through soft tissue covering the locus of bone growth, a much better performance of the electric power source can be expected due to a comparatively high capacity immediately adjacent to the bone. Through an engineered layered coating system, consisting of a succession of bioinert conductive Ti6Al4V alloy substrate/ /bioinert dielectric titania bond coat/ /electrically conducting bioactive Na:CaTiZr<sub>3</sub>(PO<sub>4</sub>)<sub>6</sub> coatings, a device with the equivalent circuit of a capacitor will be formed. The electric field strength can be optimized by simultaneously increasing the surface area of the conductor and decreasing their separation distance, i.e., decreasing the thickness of the dielectric titania layer. The surface area of the Ti6Al4V implant can be increased by appropriate grit blasting, whereas an increase of the CaTiZr<sub>3</sub>(PO<sub>4</sub>)<sub>6</sub> surface area can be obtained through engineering its porosity, for example by applying suspension or solution precursor plasma spraying techniques. Variation in porosity of the dielectric titanium oxide layer will affect the dielectric permittivity, which can be tuned to the demand.

Higher ionic conductivity of Ca (Ti,Zr) hexaorthophosphates may be achieved by aliovalent doping with highly mobile Na or Li ions intercalated into only partially occupied vacancy sites of the NaSiCON structure. Such doped compounds have been previously suggested as electrode materials for solid oxide-based fuel cells (SOFCs). In addition, it should be emphasized that an electrically conducting Na-intercalated bioceramic Na:CaTiZr<sub>3</sub>(PO<sub>4</sub>)<sub>6</sub> layer is not biologically passive but rather provides an osseoconductive function that entices osteoblasts to grow into the porous coating layer and thus anchor the implant solidly to the bone.

## 9. Conclusions and Outlook

The search for novel bioceramics together with the work for improvement of existing bioceramics, including osseoconductive hydroxylapatite coatings for arthroplasty uses, take on a particularly significant role as bone stands as the primary organ requiring surgical intervention with millions of clinical cases per year worldwide. Hence, the socio-economic implications linked to the development of efficient bone substitutes are of dramatic importance and act as a powerful driving force for the development of new, more efficient and reliable, and less expensive materials as well as improved manufacturing technologies. Consequently, the quest for osseoconductive coatings with improved

adhesive and cohesive strength, prolonged lifetime, increased reliability, and better osseointegrative and corrosion-resistant functionality is high up on the agenda of worldwide research and development. However, the limited stability of hydroxylapatite and its thermal decomposition products in the body environment call for only sparingly soluble materials or hydroxylapatite-based composites with increased in vivo resorption resistance. Ceramic materials with higher stability against in vivo resorption include, for example, Ca(Ti,Zr) hexaorthophosphates with a NaSiCON (Na Superionic Conductor) structure [68,69] with much improved mechanical and chemical stability as well as ionic conductivity. Such coatings show also reasonable osseointegrative as confirmed by in vivo implant behavior in animal models [1,20,64]. Hence, it is suggested that attention should be shifted to this novel class of bioceramics for the coating of medical implants. Such a paradigmatic shift requires strict protocols for synthesis of the ceramic material [69] as well as tight control of the parameters governing the deposition process.

**Conflicts of Interest:** The author declares no conflict of interest.

## References

1. Heimann, R.B.; Lehmann, H.D. *Bioceramic Coatings for Medical Implants*; Wiley-VCH: Weinheim, Germany, 2015.
2. Heimann, R.B. The challenge and promise of low-temperature bioceramic coatings: An editorial. *Surf. Coat. Technol.* **2016**, *301*, 1–5. [CrossRef]
3. Heimann, R.B. Thermal spraying of biomaterials. *Surf. Coat. Technol.* **2006**, *201*, 2012–2019. [CrossRef]
4. Heimann, R.B. Structure, properties, and biomedical performance of osseointegrative bioceramic coatings. *Surf. Coat. Technol.* **2013**, *233*, 25–38. [CrossRef]
5. Dotinga, R. Number of Hip Replacements Has Skyrocketed: Report. WebMD, 2015. Available online: <http://www.webmd.com/arthritis/news/20150212> (accessed on 3 April 2017).
6. Wengler, A.; Nimptsch, U.; Mansky, T. Hip and knee replacement in Germany and the USA. *Deutsches Ärzteblatt* **2014**, *111*, 407–416.
7. Pabinger, C.; Geissler, A. Utilization rates of hip arthroplasty in OECD countries. *Osteoarthritis Cartilage* **2014**, *22*, 734–741. [CrossRef] [PubMed]
8. Bourlioufas, N. Orthopaedic Joint Replacement Surgery Rates Jump in Developed Nation as Population Age. Australian Society of Orthopaedic Surgeons, News + Media, 2016. Available online: <http://www.asos.org.au/> (accessed on 3 April 2017).
9. Winter Green Research: Worldwide Hip and Knee Orthopedic Surgical Implant Market Shares, Trend, Growth, Strategy, and Forecast 2016 to 2022. 2016. Available online: <http://www.medgadget.com> (accessed on 28 March 2017).
10. Taniguchi, H. Osteosynthetic Implant. U.S. Patent Appl. 20,170,071,741, 16 March 2017.
11. Moravej, M.; Mantovani, D. Biodegradable metals for cardiovascular stent application: Interests and new opportunities. *Int. J. Mol. Sci.* **2011**, *12*, 4250–4270. [CrossRef] [PubMed]
12. Hamid, H.; Coltart, J. Miracle stents—A future without restenosis. *McGill J. Med.* **2007**, *10*, 105–111. [PubMed]
13. Di Mario, C.; Griffiths, H.; Goktekin, O.; Peeters, N.; Verbist, J.A.; Bosiers, M.; Delooste, K.; Heublein, B.; Rohde, R.; Kasese, V.; et al. Drug-eluting bioresorbable magnesium stents. *J. Interv. Cardiol.* **2004**, *17*, 391–395. [CrossRef] [PubMed]
14. Poinern, G.E.J.; Brundavanam, S.; Fawcett, D. Biomedical magnesium alloys: A review of material properties, surface modifications and potential as biodegradable orthopedic implant. *Am. J. Biomed. Eng.* **2012**, *2*, 218–240. [CrossRef]
15. Heimann, R.B.; Lehmann, H.D. Recent research and patents on controlling corrosion of bioresorbable Mg alloy implants: Towards next generation biomaterials. *Recent Pat. Mater. Sci.* **2017**, *10*, 2–19. [CrossRef]
16. Razawi, M.; Fathi, M.; Savabi, O.; Beni, B.H.; Vashae, D.; Tayebi, L. Nanostructured merwinite bioceramic coating on Mg alloy deposited by electrophoretic deposition. *Ceram. Int.* **2014**, *40*, 9473–9484. [CrossRef]
17. Beniash, E.; Patel, A.J. Self-Assembled Organosilane Coatings for Resorbable Metal Medical Devices. Patent WO2,016,126,773 A1, 11 August 2016.

18. Hodgkinson, G.; Hadba, A.R. Hydrogel Coated Magnesium Medical Implants. U.S. Patent US2,0130,060,348 A1, 7 March 2013.
19. *Standard Specification for Composition of Hydroxyapatite for Surgical Implants*; ASTM F 1185-03; ASTM International: West Conshohocken, PA, USA, 2009.
20. Heimann, R.B.; Schürmann, N.; Müller, R.T. In vitro and in vivo performance of Ti6Al4V implants with plasma-sprayed osseoconductive hydroxyapatite-bioinert titania bond coat “duplex” systems: An experimental study in sheep. *J. Mater. Sci. Mater. Med.* **2004**, *15*, 1045–1052. [[CrossRef](#)] [[PubMed](#)]
21. Park, E.; Condrate, R.A. Graded coating of hydroxyapatite and titanium by atmospheric plasma spraying. *Mater. Lett.* **1999**, *40*, 228–234. [[CrossRef](#)]
22. Heimann, R.B.; Wirth, R. Formation and transformation of amorphous calcium phosphates on titanium alloy surfaces during atmospheric plasma spraying and their subsequent in vitro performance. *Biomaterials* **2006**, *27*, 823–831. [[CrossRef](#)] [[PubMed](#)]
23. Heimann, R.B. *Plasma-Spray Coating. Principles and Application*, 2nd ed.; Wiley-VCH: Weinheim, Germany, 2008.
24. Heimann, R.B. *Classic and Advanced Ceramics. From Fundamentals to Applications*; Wiley-VCH: Weinheim, Germany, 2010.
25. Reddi, A.H. Bone morphogenetic proteins: From basic science to clinical application. *J. Bone Jt. Surg. Am.* **2001**, *83A*, S1–S6. [[CrossRef](#)]
26. Manolagas, S.C. Role of cytokines in bone resorption. *Bone* **1995**, *17*, S63–S67. [[CrossRef](#)]
27. Stenport, V.J.; Olsson, B.; Morberg, P.; Törnell, J.; Johansson, C.B. Systemically administered human growth hormone improves initial stability: An experimental study in the rabbit. *Clin. Implant Dent. Relat. Res.* **2001**, *3*, 135–141. [[CrossRef](#)] [[PubMed](#)]
28. Heimann, R.B. (Ed.) *Calcium Phosphate: Structure, Synthesis, Properties and Applications*; Biochemistry Research Trends Series; Nova Science Publishers Inc.: New York, NY, USA, 2012.
29. Hench, L.L. Bioceramics. From concept to clinic. *J. Am. Ceram. Soc.* **1991**, *74*, 1487–1510. [[CrossRef](#)]
30. Hench, L.L. Genetic design of bioactive glass. *J. Eur. Ceram. Soc.* **2008**, *29*, 1257–1265. [[CrossRef](#)]
31. Willmann, G. Material properties of hydroxyapatite ceramics. *Interceram* **1993**, *42*, 206–208.
32. Callahan, T.J.; Gantenberg, J.B.; Sands, B.E. Calcium phosphate (Ca-P) coating draft guidance for preparation of Food and Drug Administration (FDA) submissions for orthopedic and dental endosseous implants. In *Characterization and Performance of Calcium Phosphate Coatings for Implants*; ASTM STP 1196; Horowitz, E., Parr, J.E., Eds.; ASTM: Philadelphia, PA, USA, 1994; pp. 185–197.
33. Wintermantel, E.; Ha, S.W. *Biokompatible Werkstoffe und Bauweisen. Implantate für Medizin und Umwelt [Biocompatible Materials and Designs. Implants for Medicine and Environment]*; Springer: Berlin/Heidelberg, Germany; Tokyo, Japan, 1996; p. 225.
34. Demnati, I.; Grossin, D.; Combes, C.; Rey, C. Plasma-sprayed apatite coatings: Review of physical-chemical characteristics and their biological consequences. *J. Med. Biol. Eng.* **2014**, *34*, 1–7. [[CrossRef](#)]
35. Filiaggi, M.J.; Coombs, N.A.; Pilliar, R.M. Characterization of the interface in the plasma-sprayed HAP coating/Ti-6Al-4V implant system. *J. Biomed. Mater. Res.* **1991**, *25*, 1211–1229. [[CrossRef](#)] [[PubMed](#)]
36. Ji, H.; Ponton, C.B.; Marquis, P.M. Microstructural characterization of hydroxyapatite coating on titanium. *J. Mater. Sci. Mater. Med.* **1992**, *3*, 283–287. [[CrossRef](#)]
37. Webster, T.J.; Ergun, C.; Doremus, R.H.; Lanford, W.A. Increased osteoblast adhesion on titanium-coated hydroxyapatite that forms CaTiO<sub>3</sub>. *J. Biomed. Mater. Res. A* **2003**, *67*, 975–980. [[CrossRef](#)] [[PubMed](#)]
38. Heimann, R.B. Novel approaches towards design and biofunctionality of plasma-sprayed osteoconductive calcium phosphate coatings for biomedical implants: The concept of bond coats. In *Trends in Biomaterials Research*; Pannone, P.J., Ed.; Nova Science Publishers Inc.: Hauppauge, NY, USA, 2007; pp. 1–80.
39. Ning, C.Y.; Wang, Y.J.; Chen, X.F.; Zhao, N.R.; Ye, J.D.; Wu, G. Mechanical performance and microstructural characteristics of plasma-sprayed biofunctional gradient HA-ZrO<sub>2</sub>-Ti coatings. *Surf. Coat. Technol.* **2005**, *200*, 2403–2408. [[CrossRef](#)]
40. *Standard Test Method for Stereological Evaluation of Porous Coatings on Medical Implants*; ASTM F1854-15; ASTM International: West Conshohocken, PA, USA, 2015.
41. Lamy, D.; Pierre, A.C.; Heimann, R.B. Hydroxyapatite coatings with a bond coat of biomedical implants by plasma projection. *J. Mater. Res.* **1996**, *11*, 680–686. [[CrossRef](#)]

42. Lima, R.S.; Marple, B.R.; Li, H.; Khor, K.A. Biocompatible Titania Thermal Spray Coating Made from Nanostructured Feedstock. Patent Application CA 2,499,202 A1, 1 September 2006.
43. Ducheyne, P.; Radin, S.; King, L. The effect of calcium phosphate ceramic composition and structure on in vitro behavior. I. Dissolution. *J. Biomed. Mater. Res.* **1993**, *27*, 5–34. [[CrossRef](#)] [[PubMed](#)]
44. Heimann, R.B. Tracking the thermal decomposition of plasma-sprayed hydroxylapatite. *Am. Mineral.* **2015**, *100*, 2419–2425. [[CrossRef](#)]
45. De Groot, K.; Klein, C.P.A.T.; Wolke, J.G.C.; de Blicck-Hogervorst, J. Plasma-spraying of calcium phosphate. In *Handbook of Bioactive Ceramics*; Yamamuro, T., Hench, L.L., Silson, J., Eds.; CRC Press: Boca Raton, FL, USA, 1990; Volume II, pp. 3–15.
46. Gross, K.A.; Walsh, W.; Swarts, E. Analysis of retrieved hydroxyapatite-coated hip prostheses. *J. Therm. Spray Technol.* **2004**, *13*, 190–199. [[CrossRef](#)]
47. Kim, H.M.; Miyazaki, T.; Kokubo, T.; Nakamura, T. Revised simulated body fluid. *Bioceramics* **2001**, *13*, 47–50. [[CrossRef](#)]
48. Graßmann, O.; Heimann, R.B. Compositional and microstructural changes of engineered plasma-sprayed hydroxyapatite coatings on Ti6Al4V substrates during incubation in protein-free simulated body fluid. *J. Biomed. Mater. Res.* **2000**, *53*, 685–693. [[CrossRef](#)]
49. Gentile, F.; Tirinato, L.; Battista, E.; Causa, F.; Liberale, C.; di Fabrizio, E.M.; Decuzzi, P. Cells preferentially grow on rough substrates. *Biomaterials* **2010**, *31*, 7205–7212. [[CrossRef](#)] [[PubMed](#)]
50. Heimann, R.B. On the self-affine fractal geometry of plasma-sprayed surfaces. *J. Therm. Spray Technol.* **2011**, *20*, 898–908. [[CrossRef](#)]
51. Taylor, C.C.; Taylor, S.J. Estimating the dimension of a fractal. *J. R. Stat. Soc. Ser. B* **1991**, *53*, 353–364.
52. Gittens, R.A.; Olivares-Navarrete, R.; Schwartz, Z.; Boyan, B.D. Implant osseointegration and the role of microroughness and nanostructures: Lessons for spine implants. *Acta Biomater.* **2014**, *10*, 3363–3371. [[CrossRef](#)] [[PubMed](#)]
53. Topić, M.; Ntsoane, T.; Hüttel, T.; Heimann, R.B. Microstructural characterisation and stress determination in as-plasma sprayed and incubated bioconductive hydroxyapatite coatings. *Surf. Coat. Technol.* **2006**, *201*, 3633–3641. [[CrossRef](#)]
54. Heimann, R.B.; Graßmann, O.; Hempel, M.; Bucher, R.; Härting, M. Phase content, resorption resistance and residual stresses of bioceramic coatings. In *Applied Mineralogy in Research, Economy, Technology, Ecology and Culture, Proceedings of the 6th International Congress on Applied Mineralogy, ICAM2000, Göttingen, Germany, 17–19 July 2000*; CRC Press: Boca Raton, FL, USA, 2000; pp. 155–158.
55. Yang, Y.C.; Chang, E. Influence of residual stress on bonding strength and fracture of plasma-sprayed hydroxyapatite coatings on Ti–6Al–4V substrate. *Biomaterials* **2001**, *22*, 1827–1836. [[CrossRef](#)]
56. Heimann, R.B.; Itiravivong, P.; Promasa, A. In vivo-Untersuchungen zur Osseointegration von Hydroxylapatit-beschichteten Ti6Al4V-Implantaten mit und ohne bioinert Titanoxid-Haftvermittlerschicht [In vivo investigation towards osseointegration of Ti6Al4V implants with hydroxyapatite coatings with and without a bioinert titania bond coat]. *BIOMaterialien* **2004**, *5*, 38–43.
57. Itiravivong, P.; Promasa, A.; Laiprasert, T.; Techapongworachai, T.; Kuptniratsaikul, S.; Thanakit, V.; Heimann, R.B. Comparison of tissue reaction and osseointegration of metal implants between hydroxyapatite/Ti alloy coat: An animal experimental study. *J. Med. Assoc. Thail.* **2003**, *86*, S422–S430.
58. Scibior, A.; Zaporowska, H.; Ostrowski, J.; Banach, A. Combined effect of vanadium (V) and chromium (III) on lipid peroxidation in liver and kidney of rats. *Chem.-Biol. Interact.* **2006**, *159*, 213–222. [[CrossRef](#)] [[PubMed](#)]
59. König, M.A.; Gautschi, O.P.; Simmon, H.P.; Filgueira, L.; Cadosch, D. Influence of vanadium 4+ and 5+ ions on the differentiation and activation of human osteoblasts. *Int. J. Biomater.* **2017**, *2017*, 9439036. [[CrossRef](#)] [[PubMed](#)]
60. Jenko, M.; Gorenšek, M.; Godec, M.; Hodnik, M.; Batič, B.S.; Donik, C.; Grant, J.T.; Dolinar, D. Surface chemistry and microstructure of metallic biomaterials for hip and knee endoprostheses. *Appl. Surf. Sci.* **2018**, *427*, 584–593. [[CrossRef](#)]
61. *Standard Test Method for Conducting Potentiodynamic Polarization Resistance Measurements*; ASTM G59-97; American Society for Testing Materials: West Conshohocken, PA, USA, 2009.

62. Sankar, M.; Suwas, S.; Balasubramanian, S.; Manivasagam, G. Comparison of electrochemical behaviour of hydroxyapatite coated onto WE43 Mg alloy by electrophoretic and pulsed laser deposition. *Surf. Coat. Technol.* **2017**, *309*, 840–848. [[CrossRef](#)]
63. Burstein, G.T. A century of Tafel's equation: 1905–2005. A commemorative issue of corrosion science. *Corros. Sci.* **2005**, *47*, 2858–2870. [[CrossRef](#)]
64. Szmukler-Moncler, S.; Daculsi, G.; Delécrin, J.; Passuti, N.; Deudon, C. Calcium-metallic phosphates: A new coating biomaterial? *Adv. Biomater.* **1992**, *10*, 377–383.
65. Reisel, G. Entwicklung von HVOF- und APS-Gespritzten Biokeramischen Schichten für die Endoprothetik [Development of Bioceramic HVOF and APS Coatings for Endoprotheses]. Master's Thesis, RWTH University Aachen, Aachen, Germany, 1996, unpublished.
66. Heimann, R.B. In vitro- and in vivo-Verhalten von osteokonduktiven plasmagespritzten Ca-Ti-Zr-Phosphat-Beschichtungen auf Ti6Al4V-Substraten [In vitro and in vivo behaviour of osseointegrative plasma-sprayed Ca-Ti-Zr phosphate coatings deposited on Ti6Al4V substrates]. *BIOMaterialien* **2006**, *7*, 29–37.
67. Heimann, R.B. Calcium (Ti, Zr) hexaorthophosphate bioceramics for electrically stimulated biomedical implant devices. A position paper. *Am. Mineral.* **2017**, in press.
68. Alamo, J. Chemistry and properties of solids with the [NZP] skeleton. *Solid State Ion.* **1993**, *63–65*, 547–561. [[CrossRef](#)]
69. Schneider, K.; Heimann, R.B.; Berger, G.G. Plasma-sprayed coatings in the system CaO-TiO<sub>2</sub>-ZrO<sub>2</sub>-P<sub>2</sub>O<sub>5</sub> for long-term stable endoprotheses. *Materialwiss. Werkstofftech.* **2001**, *32*, 166–171. [[CrossRef](#)]



© 2017 by the author. Licensee MDPI, Basel, Switzerland. This article is an open access article distributed under the terms and conditions of the Creative Commons Attribution (CC BY) license (<http://creativecommons.org/licenses/by/4.0/>).